



Effect of cellulose nanocrystals and gelatin in corn starch plasticized films



J.S. Alves^{a,*}, K.C. dos Reis^b, E.G.T. Menezes^a, F.V. Pereira^c, J. Pereira^a

^a Departamento de Ciência dos Alimentos, Universidade Federal de Lavras, Caixa Postal 3037, CEP 37200-000 Lavras, MG, Brazil

^b Departamento de Ciências Exatas, Universidade Federal de Lavras, Caixa Postal 3037, CEP 37200-000 Lavras, MG, Brazil

^c Instituto de Ciência Exatas, Universidade Federal de Minas Gerais, Av. Antônio Carlos, 6627, Pampulha, Caixa Postal 702, CEP 31270-901 Belo Horizonte, MG, Brazil

ARTICLE INFO

Article history:

Received 22 April 2014

Received in revised form 19 July 2014

Accepted 13 August 2014

Available online 3 September 2014

Chemical compounds studied in this article:

Glycerol (PubChem CID: 753)

Sulfuric acid (PubChem CID: 1118)

Water (PubChem CID: 962)

Keywords:

Biopolymers

Nanobiocomposite

Mechanical properties

Packaging

Barrier properties

RCCD

ABSTRACT

Cellulose at the nanoparticle scale has been studied as a reinforcement for biodegradable matrices to improve film properties. The goal has been to investigate the properties of starch/gelatin/cellulose nanocrystals (CNC) films. Eleven treatments were considered using RCCD (rotatable central composite design), in addition to four control treatments. For each assay, the following dependent variables were measured: water vapor permeability (WVP), thickness, opacity and mechanical properties. The microstructure and thermal properties of the films were also assessed. Increases in gelatin and CNC concentrations lead to increases in film thickness, strength and elongation at break. The films containing only gelatin in their matrix displayed better results than the starch films, and the addition of CNC had a positive effect on the assessed response variables. The films exhibited homogeneous and cohesive structures, indicating strong interactions between the filler and matrix. Films with low levels of gelatin and CNC presented the maximum degradation temperature.

© 2014 Elsevier Ltd. All rights reserved.

1. Introduction

Starch is widely used in the form of biodegradable films in varied applications because it is a renewable, abundant and inexpensive material. According to (Fakhouri et al., 2007), films produced from polysaccharides or proteins have excellent mechanical, optical and sensory properties but are sensitive to humidity and have a high water-vapor permeability coefficient. Nevertheless, this problem can be mitigated by adding plasticizers (polyols, such as glycerol, sorbitol and polyethylene glycol) or reinforcements.

Another edible and renewable raw material used in the production of biodegradable films is gelatin. Gelatin is a protein of animal origin obtained from collagen through acid or alkaline hydrolysis that is widely used in both food and pharmaceutical industries.

Gelatin preparation may or may not involve alkaline pretreatment, which converts asparagine and glutamine into their respective acids, resulting in greater viscosity. The acid pretreatment (type A gelatin) uses pig skin, whereas the alkaline pretreatment (type B gelatin) uses cattle hides and bones. All types of gelatin have similar composition, containing water, a small amount of minerals and pure connective tissue protein (Almeida & Santanta, 2010). Gelatin is primarily used as gelling agent to create transparent, elastic gels that are thermo-reversible under cooling below 35 °C (Teixeira, 2011). According to Bertan (2003), as cited by (Fakhoury et al., 2012), gelatin-based bioplastics are resistant, transparent and easy to handle.

One of the most promising technical advances in the material industry has been the development of nanobiocomposites, namely, the dispersion of nanosized filler reinforcements into a starch biopolymer matrix (Xie, Pollet, Hallet, & Averous, 2013). Cellulose is the most abundant organic compound on earth and is found in plant cell wall in association with hemicellulose and lignine. From cellulose, the natural nano-reinforcements, called cellulose nanowhiskers (CNWs) or cellulose nanocrystals (CNCs) can be obtained using a controlled sulfuric acid hydrolysis,

Abbreviations: CNWs, cellulose nanowhiskers; CNCs, cellulose nanocrystals.

* Corresponding author. Tel.: +55 35 38291660; fax: +55 35 38291401.

E-mail addresses: janyelle.alves@yahoo.com.br (J.S. Alves),

kelen.cr@yahoo.com.br (K.C. dos Reis), evandrogtmenezes@gmail.com

(E.G.T. Menezes), fabianovp@ufmg.br (F.V. Pereira), joper@dca.ufla.br (J. Pereira).

<http://dx.doi.org/10.1016/j.carbpol.2014.08.057>

0144-8617/© 2014 Elsevier Ltd. All rights reserved.

Table 1
Experimental range and levels of independent variables.

Variables	Coded variables	Variables Levels				
		– 1.41	– 1	0	+ 1	+ 1.41
Gelatin (g 100 g ⁻¹)	X ₁	6	7.16	10	12.84	14
CNC ^a (%)	X ₂	0	0.44	1.5	2.56	3

^a CNC = cellulose nanocrystals.

producing highly crystalline rod-like nanostructures (Mesquita, Donnici, & Pereira, 2010).

CNCs (cellulose nanocrystals) act as reinforcement in biodegradable polymers, interacting with the matrix mainly to favor mechanical and barrier properties (Cao, Chen, Chang, Muir, & Falk, 2008; Cao, Chen, Chang, Stumborg, & Huneault, 2008; Kaushik, Singh, & Verma, 2010; Lu, Weng, & Cao, 2006; Mathew, Thielemans, & Dufresne, 2008; Svagan, Hedenqvist, & Berglund, 2009). This change allows a broader range of usage for these materials, especially in the packaging industry. In the present experiment, a film made from corn starch and glycerol and supplemented with gelatin was developed to obtain a more cohesive matrix. CNCs were also incorporated to this film to improve mechanical, thermal and barrier properties.

2. Materials and methods

2.1. Materials

Corn starch (Amidex[®] 3001) was supplied by Corn Products Brazil S/A, glycerol was purchased from Vetec Quimica Fina Ltda. (São Paulo, Brazil) and bovine gelatin, of 180 Bloom and 30 mesh, was obtained from Gelita do Brazil Ltda. (São Paulo, Brazil).

2.2. CNC preparation

CNC was obtained according to Beck-Candanedo, Roman, and Gray (2005) with modifications according to Mesquita et al. (2010). Sulfuric acid hydrolysis of eucalyptus wood pulp was performed. Briefly, the wood pulp was ground until a fine particulate was obtained using a Willey mill. Then, 10.0 g of cellulose was added to 80.0 mL of 64 wt% sulfuric acid under strong mechanical stirring.

Hydrolysis was performed at 50 °C for approximately 50 min. After hydrolysis, the dispersion was diluted twice in water, and the suspensions were then washed using three repeated centrifuge cycles. The last washing was conducted using dialysis against deionized water until the dispersion reached pH 6.0. Afterward, the dispersions were ultrasonicated with a Cole Parmer Sonifier cell disruptor equipped with a microtip for 8 min and finally filtered using a 20 mm pore size filter.

2.3. Film preparation

The films were prepared using a casting process, which consisted of dehydrating a filmogenic solution applied on a support (Henrique, Cereda, & Sarmento, 2008). The filmogenic solutions were prepared from 3% corn starch, 20% glycerol and gelatin solution and cellulose nanocrystals (CNC) according to the experimental range as shown in Table 1.

To improve the barrier properties of the films, in each of the 11 treatment trials (T1–T11) (Table 2), two suspensions were prepared, one with corn starch and the other with gelatin. Then these two solutions were combined. The gelatin solution was prepared by hydrating gelatin with distilled water for an hour, heating in a water bath until complete solubilization and then adding glycerol from solution. The solutions with CNC were prepared by addition of CNC to glycerol at ambient temperature, and there was occurrence of

the birefringence phenomenon as observed through crossed polarizers. The solution (CNC and glycerol) was mixed with corn starch and distilled water under stirring and heating until 75.0 °C. The two suspensions, corn starch and gelatin, were mixed to create a single suspension. The mixture was cooled to room temperature and poured onto polystyrene plates, which were dried in a controlled temperature chamber at 25 °C at 50% RH in circulated air (chamber model 435314, Hotpack, Philadelphia, USA). The dried films were peeled off the casting surface and stored in polyethylene bags at 25 ± 1 °C until evaluation.

2.4. Experimental design

Eleven treatments were prepared using a 2² rotatable central composite design (RCCD), plus four control treatments, to evaluate each single matrix (starch or gelatin) films and thus to separately analyze the interaction between CNC and each matrix. The 11 treatments (T1 through T11) were designed as presented in Table 2, consisting of two independent variables, 4 factorial points, 4 axial points and 3 central points, in accordance with Rodrigues and lemma (2005).

The response-surface methodology was applied to assess the effect that the gelatin and CNC concentrations (X₁ and X₂, respectively) had on the barrier and mechanical properties of the thin films produced here. For each assay in the experimental design, the following dependent variables were measured: water vapor permeability (WVP), thickness, opacity and mechanical properties (puncture force, tensile strength and elongation at break). The results for the scanning electron microscopy (SEM), differential scanning calorimetry (DSC) and thermo gravimetric data (TG) are shown in figures and tables generated from the assay in question.

The experiments were conducted in random order, and the data were analyzed using Statistica 8.0 (Software Inc., Tulsa, OK, USA). A significance level of 10% was adopted in the standard error analysis. The polynomial used to fit the model is given in Eq. (1).

$$y = \beta_0 + \beta_1 X_1 + \beta_{11} X_1^2 + \beta_2 X_2 + \beta_{22} X_2^2 + \beta_{12} X_1 X_2 + \varepsilon \quad (1)$$

where β_0 , β_1 , β_{11} , β_2 , β_{22} , β_{12} are the regression coefficients, X₁ is the concentration of gelatin, X₂ is the concentration of cellulose nanocrystals, and ε is the standard error.

The remaining four control treatments, namely T12 (starch + glycerol), T13 (starch + glycerol + CNC), T14 (gelatin + glycerol) and T15 (gelatin + glycerol + CNC), were produced from a suspension containing starch, glycerol, gelatin, CNC and distilled water using the concentrations defined in Table 2. These four treatments were randomly produced and split into two groups, namely T12 with T13 and T14 with T15. Standard deviation was used to ascertain how close individual values were to their mean. These four treatments served as controls for all the others because the 11 treatments were prepared from the same two-matrix (starch and gelatin) mixture.

2.5. Analyses of films

2.5.1. Water vapor permeability (WVP)

The WVP of the films was measured using a Permatran-W device, model 1/50G (San Francisco, CA, USA), with an infrared

Table 2

Experimental design for corn starch/gelatin/CNC films treatment and observed data values of water vapor permeability (WVP), thickness measurements (TM), opacity (Op), puncture force (PF), tensile strength (TS) and elongation at break (EB).

Treatment	Corn starch (g 100 g ⁻¹)	Independent variables		Dependent variables					
		Gelatin (g 100 g ⁻¹)	CNC (%)	WVP (g μm/(m ² day KPa)	TM (mm)	Op	PF (N)	TS (MPa)	EB (%)
1	3	7.16 (-1)	0.44 (-1)	6.04	0.09	38.18	27.22	41.58	8.41
2	3	12.84 (1)	0.44 (-1)	5.05	0.09	37.99	27.04	46.82	11.10
3	3	7.16 (-1)	2.56 (1)	4.97	0.11	37.98	23.36	42.93	7.50
4	3	12.84 (1)	2.56 (1)	5.18	0.09	37.85	42.50	38.29	15.61
5	3	6 (-1.41)	1.5 (0)	5.17	0.09	37.45	28.31	48.17	6.98
6	3	14(1.41)	1.5 (0)	5.95	0.08	37.79	41.90	29.30	10.00
7	3	10 (0)	0 (-1.41)	4.51	0.11	37.98	32.64	40.75	7.74
8	3	10 (0)	3(1.41)	5.82	0.08	38.51	50.29	49.09	7.56
9 (CP)	3	10 (0)	1.5 (0)	4.94 ± 0.66	0.07 ± 0.01	38.47 ± 0.17	30.28 ± 4.22	42.30 ± 1.46	8.81 ± 0.46
10 (CP)	3	10 (0)	1.5 (0)	4.58 ± 0.66	0.08 ± 0.01	38.33 ± 0.17	38.07 ± 4.22	43.59 ± 1.46	9.18 ± 0.46
11 (CP)	3	10 (0)	1.5 (0)	3.67 ± 0.66	0.07 ± 0.01	38.14 ± 0.17	39.97 ± 4.22	45.21 ± 1.46	8.27 ± 0.46
12	3	0	0	4.51	0.05 ± 0.01	39.50 ± 0.29	3.40 ± 2.16	10.91 ± 6.32	1.24 ± 0.44
13	3	0	1.5	4.63	0.04 ± 0.01	38.13 ± 1.09	2.79 ± 2.30	13.21 ± 4.92	1.99 ± 0.80
14	0	10	0	7.49	0.14 ± 0.03	37.68 ± 0.15	65.43 ± 15.19	33.09 ± 5.45	27.52 ± 12.10
15	0	10	1.5	4.56	0.13 ± 0.02	37.42 ± 0.34	69.39 ± 23.18	32.28 ± 2.18	38.25 ± 7.27

CNC = cellulose nanocrystals; CP = central point; WVP = water vapor permeability; TM = thickness measurements; Op = opacity; PF = puncture force; TS = tensile strength; EB = elongation at break; T1 = 0.44% CNC = 9.1 mL CNC solution; T2 = 0.44% CNC = 14.2 mL CNC solution; T3 = 2.56% CNC = 52.98 mL CNC solution; T4 = 2.56% CNC = 82.46 mL CNC solution; T5 = 1.5% CNC = 27.37 mL CNC solution; T6 = 1.5% CNC = 51.93 mL CNC solution; T7 = 0% CNC = 0 mL CNC solution; T8 = 3% CNC = 79.30 mL CNC solution; T9 = T10 = T11 = 1.5% = 39.65 mL CNC solution.

sensor, according to the ATSM E398 standard test method (ASTM, 2003). The film sample was placed between two foil masks with an internal area of 12.6 cm², and this unit was placed into the device's diffusion cell. The following parameters were used in the analysis: temperature of 37.8 °C and controlled relative humidity of 50% (permeant) and 10% (dry side).

2.5.2. Film thickness measurements

The film thickness was measured using a digital micrometer (Instrutemp, São Paulo, Brazil) taking measurements at different positions on the film. The results were expressed in mm.

2.5.3. Film opacity

The film opacity was determined with a color spectrometer (Minolta, model CR 400, Japan), according to the Sobral (1999) method in the reflectance mode. Opacity (Op) was calculated from the relationship between the luminosity (parameter L^*) of the film superposed on the black standard (Op_{black}) and that of the film superposed on the white standard (Op_{white}) according to the following Eq. (2):

$$OP(\%) = \frac{Op_{black}}{Op_{white}} \times 100. \quad (2)$$

2.5.4. Mechanical properties

The mechanical properties of the films were determined by two tests using a texture analyzer TA.XT2i (Stable Micro System Ltd., Surrey, England) controlled by the Exponent Lite Express V.5.1.1.0 software. The size of the load cell was 30 kg.

The specimens for the tensile strength and elongation at break analyses were cut in the shape of 80 mm × 20 mm strips, and those for the puncture-force tests were cut into 30 mm × 30 mm squares. The following parameters were used in the analysis for all the thin films samples: pre-test speed of 0.8 mm s⁻¹, test speed of 0.8 mm s⁻¹, post-test speed of 10.00 mm s⁻¹. The probe used in the tensile strength and elongation at break tests was an A/TG, with 50-mm distance between the grips.

In the puncture-force test, a film support and an SMS P/5S probe (with initial distance of 15 mm) were used. The tensile strength was calculated by dividing the maximum strength by the sectional

area of the film (film width × initial thickness). Elongation at break was calculated by dividing the extension differential by the initial distance between grips. Six specimens were used in each treatment.

2.5.5. Scanning electron microscopy (SEM)

Images were obtained according to the methodology proposed by Bengtsson, Koch, and Gatenholm (2003), with some modifications, in which small film samples (~2 mm), in their cross section, were fixed on "stubs" using double-sided adhesive tape and sputter-coated with gold before observation to prevent charging and observed using an applied voltage of 20.00 kV (sputter coater FDU 010 – Balzers Union, from Liechtenstein). These samples were later analyzed using a scanning electron microscope (LEO Electron Microscopy Ltd., Cambridge, England).

2.5.6. Differential scanning calorimetry (DSC) and thermo gravimetric data (TG)

The film properties were determined by DSC using an F3 200 DSC system (Netzsch, Germany). Approximately 3 mg of film sample were cut into small pieces and placed on a sample dish. The reference was the empty dish. The thermo gravimetric data (TG) for the various films was measured at a heating rate of 10 °C min⁻¹ from 30 °C to 300 °C.

3. Results and discussion

The suspensions (T1–T11, T13 and T15) were analyzed under two crossed polarizers, and the birefringence phenomenon was observed (Fig. 1).

According to Mesquita et al. (2010), flow birefringence in whisker suspensions results from the alignment of nanoparticles and indicates the presence of isolated CNC in the dispersion.

Table 2 shows the real and coded values for the independent variables along with the results for the dependent variables (water vapor permeability, thickness, opacity, puncture strength, tensile strength and elongation at break) for the films obtained. The values for the four control treatments (T12 through T15) were obtained as the mean of six observations (Table 2).

Table 3
Results of analysis of variance (ANOVA) for water vapor permeability (WVP), thickness measurements (TM), opacity (Op), puncture force (PF), tensile strength (TS) and elongation at break (EB).

	WVP ($\text{g } \mu\text{m}/(\text{m}^2 \text{ day KPa})$)		TM (mm)		Op		PF (N)		TS (MPa)		EB (%)	
	Cf	pV	Cf	pV	Cf	pV	Cf	pV	Cf	pV	Cf	pV
β_0	4.372	0.000	0.083	0.000	38.283	0.000	32.117	0.000	44.262	0.000	7.786	0.000
β_1	-0.050	0.828	0.011	0.023	0.072	0.480	4.266	0.069	-2.770	0.152	1.191	0.060
β_{11}	0.496	0.073	0.005	0.207	-0.252	0.046	0.218	0.911	-2.287	0.224	0.806	0.165
β_2	0.115	0.631	0.007	0.099	0.051	0.621	5.607	0.032	0.577	0.746	0.541	0.335
β_{22}	0.412	0.189	0.002	0.591	-0.023	0.850	3.220	0.218	0.362	0.866	0.786	0.255
β_{12}	0.300	0.388	0.007	0.235	0.015	0.917	5.373	0.101	-2.470	0.348	0.415	0.588
R^2	0.58		0.81		0.61		0.80		0.62		0.72	
Fc	1.41		4.40		1.57		4.11		1.62		2.62	
Ft	3.45		3.45		3.45		3.45		3.45		3.45	
p	<0.10		<0.10		<0.10		<0.10		<0.10		<0.10	

WVP = water vapor permeability; TM = thickness measurements; Op = opacity; PF = puncture force; TS = tensile strength; EB = elongation at break; Cf = coefficient; pV = p value; β_0 = constant, β_1 = gelatin (linear); β_{11} = gelatin (quadratic), β_2 = cellulose nanocrystals (linear); β_{22} = cellulose nanocrystals (quadratic); β_{12} = interaction between gelatin and cellulose nanocrystals, R^2 = coefficient of determination; Fc = F calculated, Ft = F tabulated, p = significant at 10% probability.

3.1. Water vapor permeability (WVP)

Statistical analysis of the water vapor permeability results for treatments 1 through 11, at the 10% significance level, indicated that only the quadratic term of the variable for gelatin concentration was significant, and it had a positive effect. This result indicates that an increase in gelatin concentration led to a minimum point for the response variable, i.e., the smallest results for the water vapor permeability variable comprise an intermediate value that relates mainly to the central points (Table 3). In starch and gelatin films, lower permeability is more interesting because less gas diffusion through the polymeric material is desirable.

In the central region (10% gelatin and 1.5% CNC), encompassing the central points, treatments 9, 10 and 11 correspond to the desired WVP values, i.e., the smallest ones (Table 2). The decrease in water vapor permeability in these structures with nanometric particles is justified by the fact that, when such particles are perfectly dispersed in the polymeric matrix, they create a kind of labyrinth, hindering the diffusion of water vapor through the matrix (García, Ribba, Dufresne, Aranguren, & Goyanes, 2009; Ma, Jian, Chang, & Yu, 2008).

The WVP values for the control films (starch matrix – treatments T12 and T13) were close to one another. For the gelatin films (T14 and T15), the film into which CNC was incorporated (T15) displayed a lower value, which indicated a perfect dispersion of CNC in the gelatin matrix. The reduction in permeability is strongly related to a reduction in the diffusion coefficient imposed by the presence of the fibers (Kaushik et al., 2010).

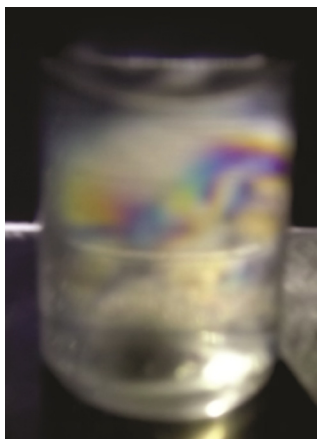


Fig. 1. Birefringence phenomenon observed between two crossed polarizers after dispersion of whiskers or cellulose nanocrystals in glycerol.

The WVP values obtained in the present work are lower than those found by Ghasemlou et al. (2013), who found results close to $8 \text{ g mm}^{-2} \text{ d}^{-1} \text{ KPa}^{-1}$ for corn starch films. The values found here are same the found for composite films based on native starches (wheat, sorghum, potato and rice) and gelatin by (Fakhouri et al., 2007) values between 4.22 and $5.53 \text{ g mm}^{-2} \text{ d}^{-1} \text{ KPa}^{-1}$.

3.2. Film thickness measurements

Table 3 lists the coefficients for the independent variables regarding the thickness of the thin films (T1 through T11). The linear terms for gelatin and CNC concentrations were significant at a 10% probability level, both being positive; i.e., an increase in the values of these variables leads to an increase in the film thickness. This behavior was expected because the gels became visually more viscous.

Given that the percentages of explained variance for thickness (R^2) were high, and the calculated F values are higher than the tabulated F , it can be concluded that the experimental data fit well to the proposed statistical model.

Eq. (3) represents the mathematical model for film thickness, where X_1 represents the gelatin concentration, and X_2 represents the CNC concentration.

$$\text{Thickness (mm)} = 0.083 + 0.011 + X_1 + 0.05X_1^2 + 0.07X_2 + 0.02X_2^2 + 0.06X_1X_2 \quad (3)$$

The analysis in Fig. 2A revealed that the lowest value for the thickness variable was reached with close to the lowest values for the gelatin concentration and intermediate levels of CNC. The films with higher thickness values (T3 and T7) displayed low values for the water vapor permeability variable (Table 2). According to Henrique et al. (2008), thickness influences film properties and, when controlled, allows for material uniformity and validity among comparisons.

The gelatin films (T14 and T15) displayed higher thickness values than the starch films (T12 and T13) (Table 2). The gelatin films were more viscous than the starch films, most likely because the gelatin concentration (10%) used was higher than in the starch films (3%). Moreover, gelatin consists mainly of protein, which may lead to higher viscosity and consequently greater thickness.

Other authors who have worked with corn starch films found thickness values of approximately 0.15 mm (Ghasemlou et al., 2013). (Fakhouri et al., 2007) assessed the thickness of composite films made with native starches from wheat, sorghum, potato, rice and gelatin and found results between 0.053 mm and 0.063 mm, which are lower than those found in the present

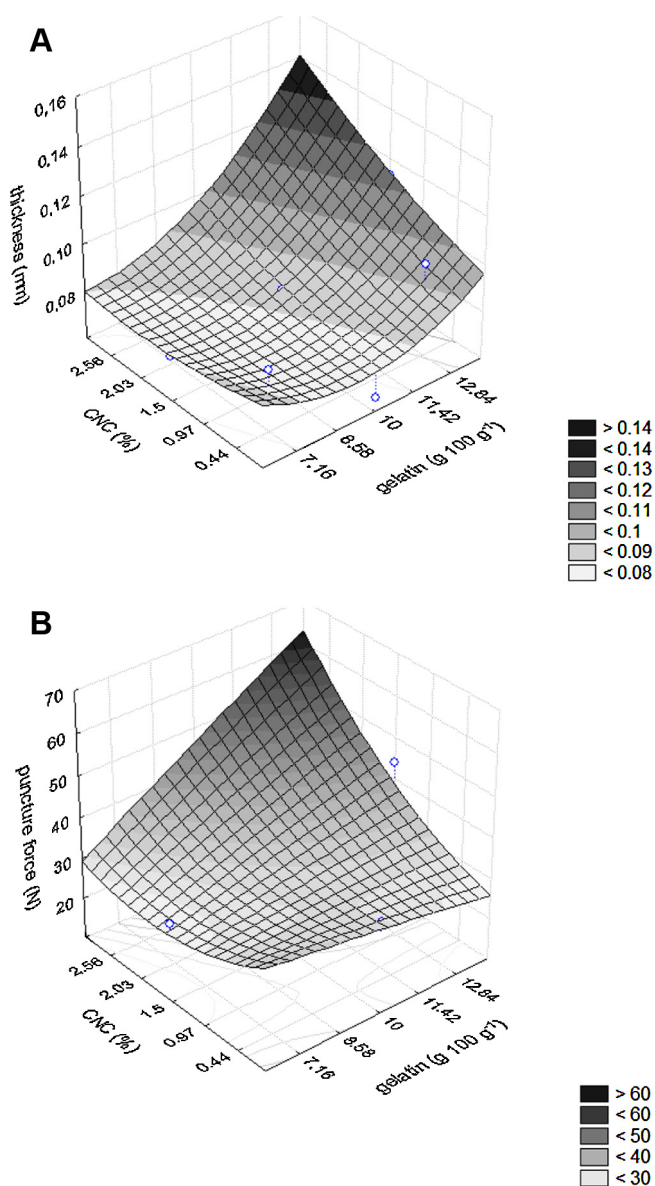


Fig. 2. Response-surface plots showing the effect of the interaction between independent variables for the (A) thickness variable (mm) and (B) puncture force variable (N) with CNC (%) versus gelatin (g 100 g⁻¹).

study. Maran, Sivakumar, Sridhar, and Thirugnanasambandham (2013) assessed cassava starch-based edible films and found values between 0.027 mm and 0.046 mm for film thickness.

3.3. Film opacity

Only the quadratic term for gelatin concentration was significant at a 10% probability level, displaying a negative value (Table 3). The increase in gelatin concentration led to an increase in opacity until maximum values were reached. Table 2 for factorial design indicates that the highest opacity values were obtained in the treatments with intermediate values of gelatin concentration in the film compositions (T8, T9, T10 and T11). Because the opacity is inversely proportional to the transparency, the treatments suggested in this study would be those displaying the lowest opacity values, namely treatments 5 and 6. According to Chen, Kuo, and Lai (2010) the transparency of films is relatively important when films will be used for food packaging or food coating because this factor directly influences consumer acceptability.

The opacity is highly influenced by the crystalline content of a sample: more compact polymer chains make it more difficult for light pass through and increase the opacity of films (Matsuguma et al., 2009 cited by Fakhouri et al., 2013). Comparison of the results for control films T12, T13, T14 and T15 reveals that the lowest values were found in gelatin films and, among them (T12, T13) (T14, T15), the films with CNC displayed lower values. This fact may be an indication that nanoparticles were homogeneously distributed in the matrix because they are white, and light incident on the film surface is reflected in larger quantity due to the white particles.

Chen, Liu, Chang, Cao, and Anderson (2009) report that nanocomposite films display higher transparency than pure-starch films due to the nanometer size, the homogeneous dispersion and the strong interaction between nanowhiskers and the starch matrix.

3.4. Mechanical properties

According to Table 3, the linear terms gelatin concentration and CNC were significantly ($p < 0.10$) and positively correlated. This result indicates that increasing gelatin concentration and CNC (%) drive an increase in the puncture force. This behavior is desirable because a greater required puncture force indicates greater film resistance, and resistant film is better suited for applications in the packaging and coating industries.

The percentage of explained variance for the puncture force was high (80%), and because the values for F_{calc} (4.11) are higher than F_{tab} (3.45), the model appears to fit well to the experimental data.

Eq. (4) represents the mathematical model for the puncture force of the films, where X_1 represents the gelatin concentration, and X_2 represents the CNC concentration.

$$\text{Puncture force (N)} = 32.117 + 4.266X_1 + 0.218X_1^2 + 5.607X_2 + 3.220X_2^2 + 5.373X_1X_2. \quad (4)$$

Based on the proposed model, a response surface was generated. The best results for the puncture force are obtained with treatments that had the highest gelatin and CNC concentration values (Fig. 2B), which according to the factorial design in Table 2 are treatments 4, 6 and 8.

For the control films, higher puncture force was observed in gelatin films (T14 and T15) than in starch films (T12 and T13). Analysis of the gelatin films separately showed that the addition of CNC increased the required puncture force.

These results are in agreement with the WVP analysis, in which the same behavior was observed because these films exhibited lower permeability. This behavior can be an indication that the CNC dispersion was more homogenous in the gelatin matrix. A high level of nanofiller addition can adversely affect the film properties because of aggregation (Chen, Liu, Chang, Anderson, & Huneault, 2009).

In general, the results for puncture force of starch/gelatin films found in this work (Table 2) were higher than those found in the experiment by Aguilar-Méndez, Martín-Martínez, Tomás, Cruz-Orea, and Jaime-Fonseca (2008) (11.3 N–32.6 N), in which the physicochemical properties of starch/gelatin films were assessed.

Table 3 shows that no term was significant at a 10% probability level for the tensile strength variable. For this type of film, higher tensile strengths are better because this property is related to the ultimate tensile strength, i.e., the maximum stress that the film can withstand without becoming deformed.

According to Table 2, the best values for tensile strength were found in treatments 5 and 8.

For the control films, the gelatin films T14 and T15 had greater tensile strength than the starch films T12 and T13.

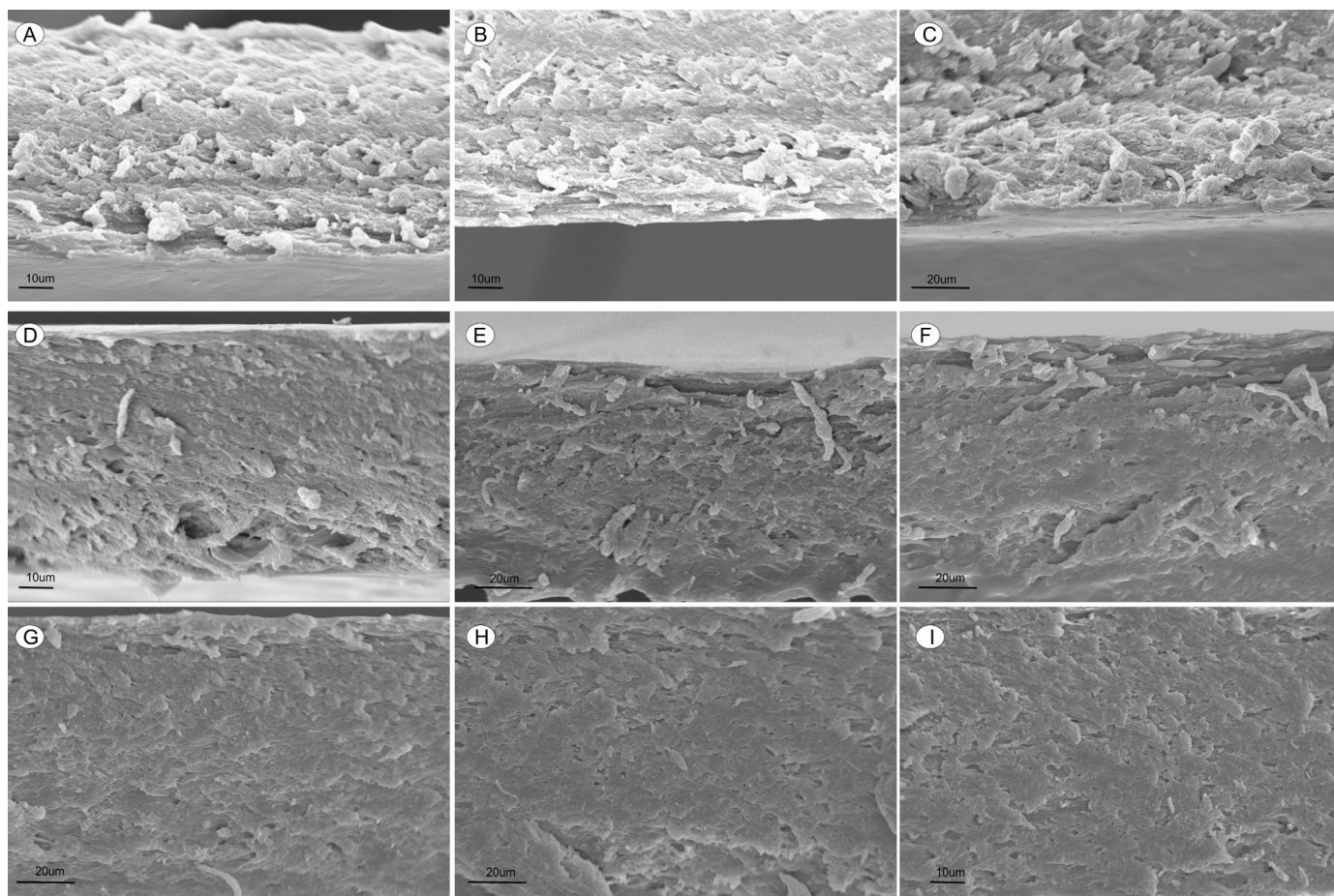


Fig. 3. Cross-section micrographs of thin films observed by SEM, where (A) treatment 1, (B) treatment 2, (C) treatment 3, (D) treatment 4, (E) treatment 5, (F) treatment 6, (G) treatment 7, (H) treatment 8, (I) treatment 9.

Fakhouri et al. (2007) found values between 56.24 MPa and 104.62 MPa for composite films based on native starches (wheat, sorghum, potato and rice) and gelatin, which higher than the values found in the present study.

Table 3 shows that only the linear term of gelatin concentration was significant at a 10% probability level, and its effect was positive. This pattern means that the addition of gelatin to treatments increased their elongation at the breaking point, and higher values of this variable are better for application of these films for food coating and packaging.

Although the CNC concentration variable was not significant, treatment 4 displayed the highest result for elongation at break (Table 2). This treatment had higher concentrations of gelatin and CNC than the control treatments.

Regarding the control films, the gelatin T14 and T15 displayed higher values for elongation at break than the starch films T12 and T13. Remembering that all films have the same amount of glycerol plasticizer, the comparison between the starch film (comparing T12 with T13 treatments) and gelatin films (comparing T14 with T15 treatments), showed that the incorporation of CNC increased the elongation at break values. This result of increase in the elongation at break is somewhat unexpected, but other authors have also found similar results for PLA/CNCs nanocomposites plasticized with PEG (Oksman, Mathew, Bondeson, & Kvien, 2006) and for starch/CNCs plasticized with sorbitol (Kvien, Sugiyama, Votrubec, & Oksman, 2007). Oksman et al. (2006) found a clear positive effect on the elongation at break of the nanocomposites with the addition of CNCs with PEG. The composites PLA/CNCs/PEG presented

a considerable increase in the elongation at break compared with the system without CNCs (PLA/PEG). This somewhat unexpected result was explained through a combination of nano-sized CNCs dispersed together with a plasticizer (PEG). Since the CNCs present a polar and high surface area that can interact strongly with a polar plasticizer (such as PEG or glycerol), the authors stated that PEG interacts strongly with the CNCs, covers them and improve the dispersion of the nanoparticles. Additionally, the plasticizer can be more dispersed in the presence of the cellulose nanoparticles. We believe that this effect can be the reason for the increase in the elongation at break observed with the addition of the CNCs in a combination with the plasticizer in our case.

3.5. Scanning electron microscopy (SEM)

Fig. 3 shows cross section photomicrographs of the thin films made with corn starch, glycerol, gelatin and CNC at 500× magnification. The films were frozen in liquid nitrogen and broken into small pieces.

In general, the thin films have a homogenous appearance, i.e., uniform interactions between the filler (CNC) and matrix (starch or gelatin).

The corn-starch/gelatin thin films were less compact at lower gelatin and/or CNC concentrations compared to the films with intermediate to high gelatin and/or CNC concentrations (Fig. 3F–I – central point). The latter films displayed a more compact texture. However, Fig. 3I stands out from the rest. According to Henrique et al. (2008), that work with casting films, the presence of pores

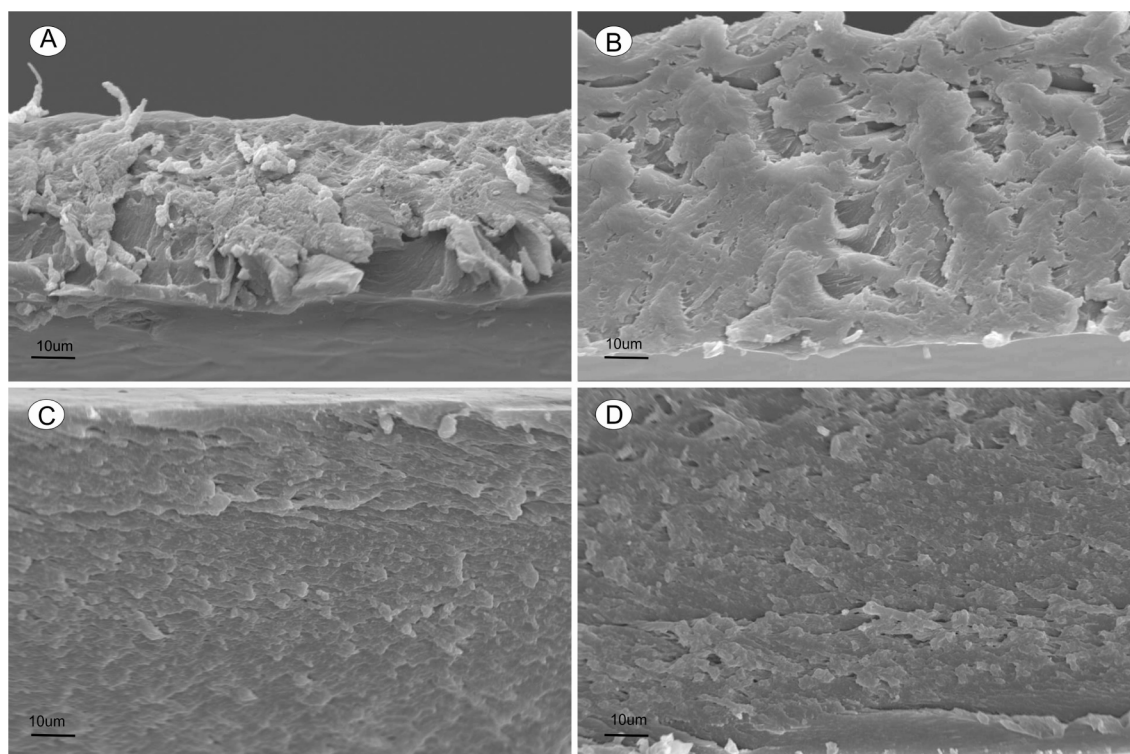


Fig. 4. Cross-section micrographs of thin films – control, observed by SEM, where (A) treatment 12, (B) treatment 13, (C) treatment 14, (D) treatment 15.

may influence permeability, and, as mentioned above and in agreement with the WVP results for the intermediate concentrations (10% gelatin and 1.5% CNC; treatments 9, 10 and 11), the lowest values were found at the central points, exactly where the desired values for WVP were. This result confirmed that the structure was more compact.

It is important to mention that the treatment 4 (Fig. 3D) exhibited small empty spaces inside the formed matrix due to the process by which the film was produced (i.e. mixing of the suspension at high rotation, favoring the formation of air micro bubbles). For this reason, even though that apparently the presence of these micro bubbles did not provide a significant effect on the WVP and mechanical properties for this treatment (compared to the other films), it is difficult to affirm that the behavior observed for this film is undoubtedly from the formulation.

The photomicrographs of the gelatin control films (Fig. 4C and D) reveal that these films had a more compact appearance and greater thickness than the corn-starch control films (Fig. 4A and B). This difference can be confirmed by the results of the thickness analysis conducted in this work (Table 2). This more compact appearance and greater thickness resulted in films that were more resistant (higher values for puncture force and tensile strength) as shown in the results for the tested mechanical properties (Table 2).

3.6. Differential scanning calorimetry (DSC) and thermo gravimetric data (TG)

Based on Differential scanning calorimetry (DSC), the gelatin and nanofiber addition altered the melting (gelatinization) peak

Table 4

Peak temperatures of melting (T_p), the onset of melting point (T_o) and the conclusion temperatures of the same transition (T_c) obtained from DSC and Thermo Gravimetric (TG) data of the films, showing the onset (T_o) and maximum degradation (T_{max}) temperatures of the samples.

Treatment	DSC			TG	
	T_p (°C)	T_o (°C)	T_c (°C)	T_o (°C)	T_{max} (°C)
1	95.41	46.69	147.16	286.68	298.47
2	56.39	51.93	115.38	262.24	296.73
3	78.85	49.39	146.27	284.50	296.58
4	91.36	51.03	152.10	275.36	296.97
5	76.78	51.16	182.94	291.77	296.88
6	72.05	51.19	155.61	–	–
7	73.11	51.98	138.88	264.18	296.39
8	104.40	50.17	178.57	269.36	296.90
9	61.60	45.43	118.48	304.13	296.84
10	84.61	48.73	152.10	263.36	296.79
11	88.56	41.75	158.00	276.06	296.83
12	56.18	45.16	121.26	–	–
13	55.95	50.82	132.66	288.10	297.28
14	97.13	46.90	135.10	254.28	296.66
15	170.18	51.62	176.05	248.34	296.78

DSC (Differential scanning calorimetry) – transition temperatures; T_p = peak temperatures of melting; T_o = onset of melting point; T_c = conclusion temperatures of melting; TG = thermo gravimetric data of films; T_o = onset degradation temperatures; T_{max} = maximum degradation temperatures.

temperature (T_p), the onset of melting (T_o) and the endset (T_c) of the same transition (Table 4).

The films prepared with starch alone or only with the addition of CNCs in the starch matrix (treatments 12 and 13) presented the lowest values of T_p (gelatinization temperatures of starch) around 56 °C. The addition of gelatin altered significantly the T_p values, but not significantly the onset temperature of melting point for all treatments.

The thermal stability of the materials was investigated by thermogravimetric analysis, and the effect of the gelatin and CNC concentration on the thermal properties of the starch films was also studied. The temperature corresponding to the maximum rate of weight loss (T_{max}) and the onset temperature (T_0) of the films are presented in Table 4.

The films with low contents of gelatin and of CNC presented the maximum degradation temperature (298.47 °C). According to some authors (Chen, Liu, Chang, Anderson, et al., 2009; Chen, Liu, Chang, Cao, et al., 2009; Kaushik et al., 2010), adding CNWs to a starch matrix may reduce the thermal stability.

4. Conclusion

Based on the experimental design employed in this work (RCCD), in general, the independent variable gelatin interfered in the analyzed film properties by increasing the values found. For the response variable of water vapor permeability, the intermediate gelatin concentration led to the lowest value. For the thickness, puncture force and elongation at break variables, increasing the gelatin and CNC concentrations increased the values found. Regarding the control films, the films containing a gelatin-only matrix displayed better results than starch matrices for opacity and mechanical properties. Moreover, comparisons between the films of a given matrix regarding the addition of CNC showed that CNC had a positive effect on the response variables measured. The mechanical properties of the studied films enhanced significantly with the concentration of gelatin and CNCs within the corn starch films. The films with low contents of gelatin and of CNC presented the maximum degradation temperature.

Acknowledgments

The authors thank the Brazilian Federal Agency for Support and Evaluation of Graduate Education (Coordenação de Aperfeiçoamento de Pessoal de Nível Superior – CAPES), the National Counsel of Technological and Scientific Development (Conselho Nacional de Desenvolvimento Científico e Tecnológico – CNPq) and the Minas Gerais Research Foundation (Fundação de Amparo à Pesquisa do estado de Minas Gerais – FAPEMIG) for their financial support.

References

Aguilar-Méndez, M. A., Martín-Martínez, E. S., Tomás, S. A., Cruz-Orea, A., & Jaime-Fonseca, M. R. (2008). Gelatine–starch films: Physicochemical properties and their application in extending the post-harvest shelf life of avocado (*Persea americana*). *Journal of the Science of Food and Agriculture*, 88, 185–193.

Almeida, P. F. D., & Santanta, J. C. C. (2010). Avaliação da qualidade de uma gelatina obtida a partir de tarsos de frango. In XXX Encontro Nacional de Engenharia de Produção (XXX National Meeting of Production Engineering) São Carlos. Available at: <http://www.abepro.org.br/biblioteca/enegep2010.TN.STP.114.750.15403.pdf> Accessed 6.02.14

ASTM. (2003). Designation E 398 – 03: Standard test method for water vapor transmission rate of sheet materials using dynamic Relative humidity measurement. In *Annual book of ASTM standards*. Philadelphia: American Society for Testing and Materials.

Beck-Candanedo, S., Roman, M., & Gray, D. G. (2005). Effect of reaction conditions on the properties and behavior of Wood cellulose nanocrystal suspensions. *Biomacromolecules*, 6, 1048–1054.

Bengtsson, M., Koch, K., & Gatenholm, P. (2003). Surface octanoylation of high-amylose potato starch films. *Carbohydrate Polymers*, 54, 1–11.

Cao, X., Chen, Y., Chang, P. R., Muir, A. D., & Falk, G. (2008). Starch-based nanocomposites reinforced with flax cellulose nanocrystals. *Express Polymer Letters*, 2, 502–510.

Cao, X., Chen, Y., Chang, P. R., Stumborg, M., & Huneault, M. A. (2008). Green composites reinforced with hemp nanocrystals in plasticized starch. *Journal of Applied Polymer Science*, 109, 3804–3810.

Chen, Y., Liu, C., Chang, P. R., Anderson, D. P., & Huneault, M. A. (2009). Pea starch-based composite films with pea hull fibers and pea hull fiber-derived nanowhiskers. *Polymer Engineering & Science*, 49, 369–378.

Chen, Y., Liu, C., Chang, P. R., Cao, X., & Anderson, D. P. (2009). Bionanocomposites based on pea starch and cellulose nanowhiskers hydrolyzed from pea hull fibre: Effect of hydrolysis time. *Carbohydrate Polymers*, 76, 607–615.

Chen, C. H., Kuo, W. S., & Lai, L. S. (2010). Water barrier and physical properties of starch/decolorized Hsian-tsao leaf gum films: Impact of surfactant lamination. *Food Hydrocolloids*, 24, 200–207.

Fakhouri, F. M., Fontes, L. C. B., Gonçalves, P. V., de, M., Milanez, C. R., Steel, C. J., et al. (2007). Films and edible coatings based on native starches and gelatin in the conservation and sensory acceptance of crimson grapes. *Ciência e Tecnologia de Alimentos*, 27, 369–375.

Fakhouri, F. M., Costa, D., Yamashita, F., Martelli, S. M., Jesus, R. C., Alganer, K., et al. (2013). Comparative study of processing methods for starch/gelatin films. *Carbohydrate Polymers*, 95, 681–689.

Fakhoury, F. M., Martelli, S. M., Bertan, L. C., Yamashita, F., Innocentini Mei, L. H., & Collares Queiroz, L. H. (2012). Edible films made from blends of manioc starch and gelatin – influence of different types of plasticizer and different levels of macromolecules on their properties. *LWT – Food Science and Technology*, 49, 149–154.

García, N. L., Ribba, L., Dufresne, A., Aranguren, M. I., & Goyanes, S. (2009). Physico-mechanical properties of biodegradable starch nanocomposites. *Macromolecular Materials and Engineering*, 294, 169–177.

Ghasemlou, M., Aliheidari, N., Fahmi, R., Shojaee-Aliabadi, S., Varz, B. K., Cran, M. J., et al. (2013). Physical, mechanical and barrier properties of corn starch films incorporated with plant essential oils. *Carbohydrate Polymers*, 98, 1117–1126.

Henrique, C. M., Cereda, M. P., & Sarmento, S. B. S. (2008). Características físicas de filmes biodegradáveis produzidos a partir de amidos modificados de mandioca [Physical characteristics of cassava modified starch films]. *Ciência e Tecnologia de Alimentos*, 28, 231–240.

Kaushik, A., Singh, M., & Verma, G. (2010). Green nanocomposites based on thermoplastic starch and steam exploded cellulose nanofibrils from wheat straw. *Carbohydrate Polymers*, 82, 337–345.

Kvien, I., Sugiyama, J., Votruba, M., & Oksman, K. (2007). Characterization of starch based nanocomposites. *Journal of Materials Science*, 42, 8163–8171.

Lu, Y., Weng, L., & Cao, X. (2006). Morphological, thermal and mechanical properties of ramie crystallites – reinforced plasticized starch biocomposites. *Carbohydrate Polymers*, 63, 198–204.

Ma, X., Jian, R., Chang, P. R., & Yu, J. (2008). Fabrication and characterization of citric acid-modified starch nanoparticles/plasticized-starch composites. *Biomacromolecules*, 9, 3314–3320.

Maran, J. P., Sivakumar, V., Sridhar, R., & Thirugnanasambandham, K. (2013). Development of model for barrier and optical properties of tapioca starch based edible films. *Carbohydrate Polymers*, 92, 1335–1347.

Mathew, A. P., Thielemans, W., & Dufresne, A. (2008). Mechanical properties of nanocomposites from sorbitol plasticized starch and tunicin whiskers. *Journal of Applied Polymer Science*, 109, 4065–4074.

Mesquita, J. P. D., Donnici, C. L., & Pereira, F. V. (2010). Biobased nanocomposites from layer-by-layer assembly of cellulose nanowhiskers with chitosan. *Biomacromolecules*, 11, 473–480.

Oksman, K., Mathew, A. P., Bondeson, D., & Kvien, I. (2006). Manufacturing process of cellulose whiskers/poly(lactic acid) nanocomposites. *Composites Science and Technology*, 66, 2776–2784.

Rodrigues, M. I., & Iemma, A. F. (2005). (*Experimental design and process optimization: A sequential design strategy*) Planejamento de experimentos e otimização de processos: Uma estratégia seqüencial de planejamentos (1st ed.). Campinas, SP: Casa do Pão Editora.

Sobral, P. J. A. (1999). Propriedades funcionais de biofilmes de gelatina em função da espessura [Functional properties of gelatin biofilms as a function of thickness]. *Ciência e Engenharia*, 8, 60–67.

Svagan, A. J., Hedenqvist, M. S., & Berglund, L. (2009). Reduced water vapour sorption in cellulose nanocomposites with starch matrix. *Composites Science and Technology*, 69, 500–506.

Teixeira, A. M. (2011). (*Nanocomposites of montmorillonite clay, thermoplastic starch, gelatin, soy protein isolate and chitosan*) Nanocompósitos de argila montmorilonita, amido, gelatina, isolado protéico de Soja e quitosana (Ph.D. thesis). Campinas, SP: Universidade Estadual de Campinas.

Xie, F., Pollet, E., Halley, P. J., & Averous, L. (2013). Review: Starch-based nanobio-composites. *Progress in Polymer Science*, 38, 1590–1628.